REFINEMENT OF THE STRUCTURE OF CUBANITE, $CuFe_2S_3$

LEONID V. AZAROFF* AND M. J. BUERGER, *Crystallographic Laboratory, Department of Geology and Geophysics, Massachusetts Institute of Technology.*

ABSTRACT

The structure of cubanite, $CuFe_2S_3$, was known from an earlier trial-and-error investigation. In this structure both iron and copper atoms are tetrahedrally coordinated to sulfur. The structure is peculiar in that the Fe tetrahedra share an edge giving rise to a short Fe-Fe distance which probably corresponds to a bond. Because of the ferromagnetism of cubanite it is important to know the details of the structure with accuracy. To this end the refining of the structure is herewith reported. The refining process was carried out in three stages: (1) by electron density projections, (2) by plane sections through the three-dimensional distribution of electron density, and (3) by difference line syntheses, ρ_o-ρ_c through each atom. In the refined structure, the Fe atoms are found to be coordinated to four S atoms at distances of 2.29, 2.28, 2.27, 2.25 Å, and one Fe atom at 2.81 Å. The shared tetrahedral edge is somewhat shortened, having a length of 3.61 Å, as compared with the other edges of 3.71, 3.72, 3.73, 3.84, and 3.84 Å.

INTRODUCTION

The crystal structure of cubanite was determined by M. J. Buerger (1945, 1947). The metal atoms in this structure are tetrahedrally surrounded by sulfur atoms. The structure can be briefly described as slabs of the wurtzite arrangement parallel to (010) and averaging b/2 wide. These wurtzite-like slabs are joined to one another by inversion centers so that neighboring slabs have their tetrahedral apices reversed. The central portion of each slab is composed of copper tetrahedra and the sides of this slab are composed of iron tetrahedra. Since the inversion center occurs at a midpoint of an edge of an iron tetrahedron, it has the effect of joining all iron tetrahedra in pairs which share this edge. The sharing of tetrahedral edges is unusual, even in non-ionic crystals. It was only reasonable to suppose that the close approach of iron atoms across the shared tetrahedral edge corresponds to an Fe-Fe bond. This suggested that the iron atoms, in addition to being bonded to four sulfur atoms, are also bonded to one another in pairs.

Cubanite is one of the two ferromagnetic sulfide minerals. It has been suggested (Buerger, 1945) that the ferromagnetism may be related to the unusual coordination of iron. For this reason a detailed knowledge of the bond distances in cubanite is of more than routine interest. The original structure determination was carried out by trial-and-error methods, and, due to the limitations of the method, the accuracy of the

* Now with the solid-state section of the Armour Research Foundation, Chicago, Illinois.

published coordinates of the atoms is not known. Because of the bearing of the interatomic distances on the theory of ferromagnetism in cubanite, a refinement of the parameters of the structure was regarded as important. The details and results of the refinement investigation are reported here.

The space group of cubanite is *Pcmn*. The cell dimensions are as follows:

$$a = 6.46\ \text{Å}$$
$$b = 11.12$$
$$c = 6.23$$

This cell contains $4CuFe_2S_3$. The best coordinates found by the original trial-and-error search were as follows:

	x	y	z
Cu in 4*c*:	$\sim\frac{7}{12}$	$(\frac{1}{4})$	.122
S_I in 4*c*:	$\sim\frac{11}{12}$	$(\frac{1}{4})$	.270
Fe in 8*d*:	$\sim\frac{1}{12}$	.083	.135
S_{II} in 8*d*:	$\sim\frac{5}{12}$	.083	.265

Experimental Procedure

Intensity determination. One of the crystals from the Frood Mine, Sudbury, Ontario, used for the original structure determination, was selected for intensity measurement. The crystal was mounted with its *b* axis parallel to the axis of the goniometer head and set on the precession (Buerger, 1944) camera. This mounting made it possible to take photographs of the *hk*0 and 0*kl* reflections with one mounting of the crystal. These reflections were recorded for MoK_α radiation and the intensities were measured by using the M.I.T. modification of the Dawton (1938) method.

For crystals having orthorhombic symmetry, the entire three-dimensional reciprocal lattice can be recorded by the precession apparatus with a single mounting of the crystal. This is illustrated in Fig. 1. To accomplish this, one records zero and upper levels normal to the *a* and *c* axes as far as the range of the apparatus permits. The reflections missing due to the blind spot of the upper levels, and the reflections missing because they occur on the higher levels normal to each axis, are filled in by photographing the series of levels normal to $[\bar{1}01]$.

The symmetry of the reciprocal lattice combined with the repeated

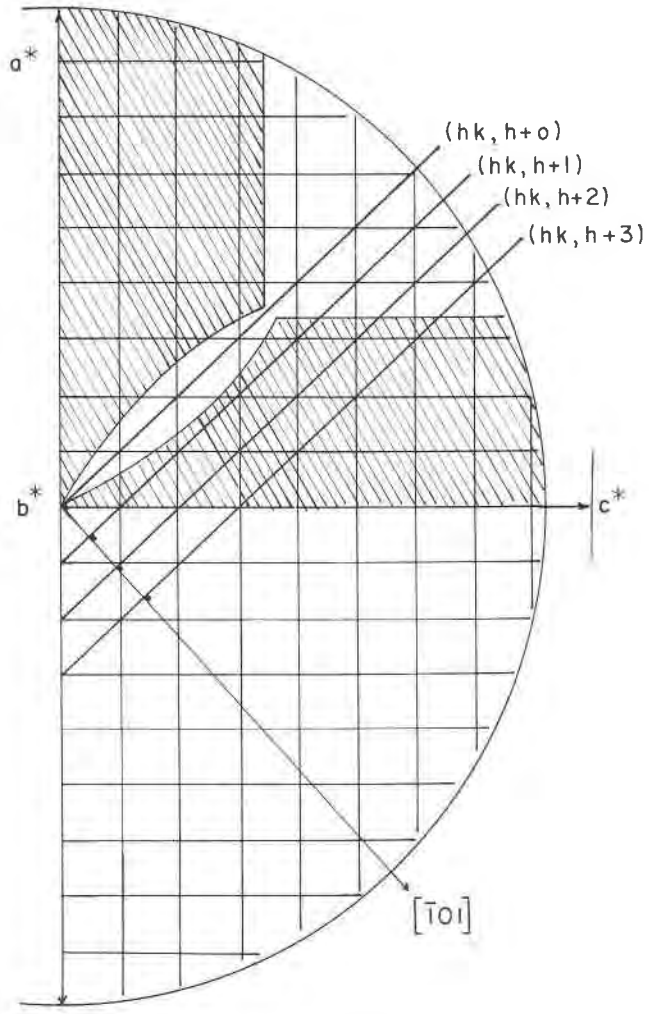

FIG. 1. Projection of reciprocal lattice of cubanite, showing regions explorable by precession photographs. Shaded areas are regions explorable by *a* axis and *c* axis precession photographs. Additional lines show how blind regions of *a* axis and *c* axis photographs can be filled in by [$\bar{1}$01] axis precession photographs.

appearance of the same spots on more than one photograph provided the possibility of making four independent measurements of approximately 70% of the observable intensities. The remaining intensities were measured independently at least twice. The averages of these measurements were then used as the final observed intensities.

Correction of intensity. The intensities were corrected by applying the

Lorentz and polarization factors as determined for the zero-level precession photographs by Waser (1951) and upper levels by Burbank (1952) and Grenville-Wells and Abrahams (1952). The charts prepared by the above-mentioned authors were enlarged to a scale of 1 reciprocal lattice unit = 10 cm. and printed on transparent film. These films were then placed over a reciprocal-lattice net drawn to the same scale. The use of these enlarged charts and reciprocal-lattice nets rather than the original films allows a more accurate and rapid determination of the value of the correction.

The intensities were next corrected for absorption by the crystal. Since the crystal was an irregular, jagged fragment, an exact determination of the absorption correction was nearly impossible. An approximate

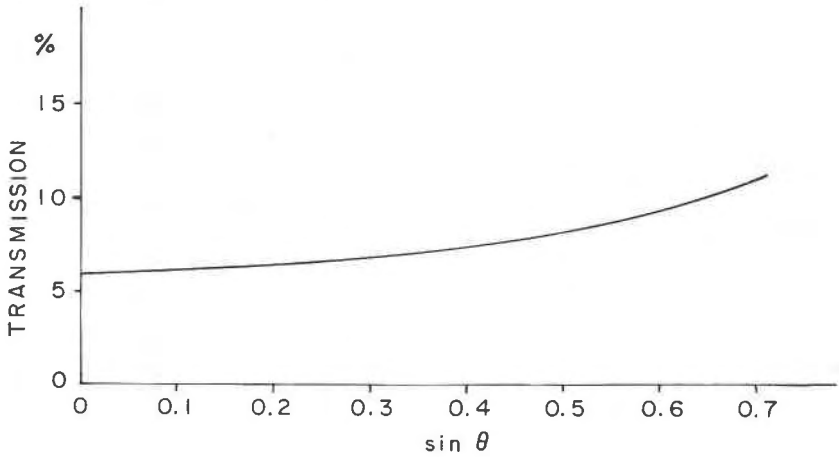

FIG. 2. Transmission of Mo$K\alpha$ radiation by cubanite crystal used.

absorption correction based on the assumption that the crystal was spherical was therefore applied. Although this assumption is not strictly valid, it was felt that such an absorption correction would, nevertheless, appreciably decrease the errors in the observed intensities due to absorption effects.

The absorption corrections made were based on a method suggested by Ekstein and Evans (1951). The radius r of the sphere is first determined. In this case the average radius of the crystal ($r = 0.0175$ cm.) was used. The value of the radius is then multiplied by the linear absorption coefficient of the crystal, in this case $\mu = 127.5$ cm^{-1}. The per cent transmission as a function of θ can then be determined by forming the product $\mu r = 2.23$, and referring to the above-cited tables. The tables list the per cent of x-radiation transmitted at the angles $\theta = 0°$, $22\frac{1}{2}°$, $45°$, $67\frac{1}{2}°$ and

90°. These values are then plotted and the best curve drawn through them. In this case the plot of transmissivity was made against sin θ rather than θ as suggested by Evans (Ekstein and Evans, 1951), and is shown in Fig. 2. The absorption correction was then applied to the observed intensities by reading the per cent transmitted corresponding to the value of sin θ for the reflection concerned and dividing the observed intensity by this value.

Finally, the square roots of the corrected intensities were taken and these values were used as the observed structure factors. The observed structure factors were placed on an absolute basis by plotting $|F_o|/|F_c|$ against $\sin^2\theta$, Fig. 6. This plot not only determined the scale of the $|F_o|$'s but also the temperature factor ($B=1.63$) which was applied to the computed structure factors.

Refinement of Coordinates

Outline of refinement procedure. The refinement was carried out in three stages. The first stage consisted of refinement by the electron-density

Table 1. Coordinates of Atoms in Cubanite at Various Stages of Refinement

Atom	Coordinates Determined by									
	Original Trial-and-error Determination	$\rho(yz)$		$\rho(x\frac{1}{4}z)$ and $\rho(x\frac{1}{12}z)$		First Difference Synthesis		Second Difference Synthesis		Parameters Finally Accepted
		Initial	Final	Initial	Final	Initial	Final	Initial	Final	
	$\frac{1}{12}$			.083$_5$	.085	.085	.087$_5$	.087$_5$	.087$_5$	.087$_5$
Fe y	.083	.083	.085			.085	.088	.088	.088	.088
z	.135	.135	.136	.136	.133	.133	.134	.134	.134	.134
	$\frac{7}{12}$			.583	.583	.583	.583	.583	.583	.583
Cu y	$\frac{1}{4}$	$\frac{1}{4}$	$\frac{1}{4}$			$\frac{1}{4}$	$\frac{1}{4}$	$\frac{1}{4}$	$\frac{1}{4}$	$\frac{1}{4}$
z	.122	.122	.124	.124	.125	.125	.127	.127	.127	.127
	$\frac{11}{12}$			.916	.914	.914	.913	.913	.913	.913
S$_{\text{I}}$ y	$\frac{1}{4}$	$\frac{1}{4}$	$\frac{1}{4}$			$\frac{1}{4}$	$\frac{1}{4}$	$\frac{1}{4}$	$\frac{1}{4}$	$\frac{1}{4}$
z	.270	.270	.264	.264	.263	.263	.262	.262	.262$_5$	.262$_5$
	$\frac{5}{12}$			.417	.415	.415	.413	.413	.413	.413
S$_{\text{II}}$ y	.083	.083	.084			.084	.083$_5$	.083$_5$	.083$_5$	.083$_5$
z	.265	.265	.274	.274	.274	.274	.274	.274	.274	.274
R:	22% $0kl$	9.7% $hk0$ 19 % $0kl$		14% hkl		7.7% $hk0$ 11 % $0kl$		11.9% hkl		11.9% hkl

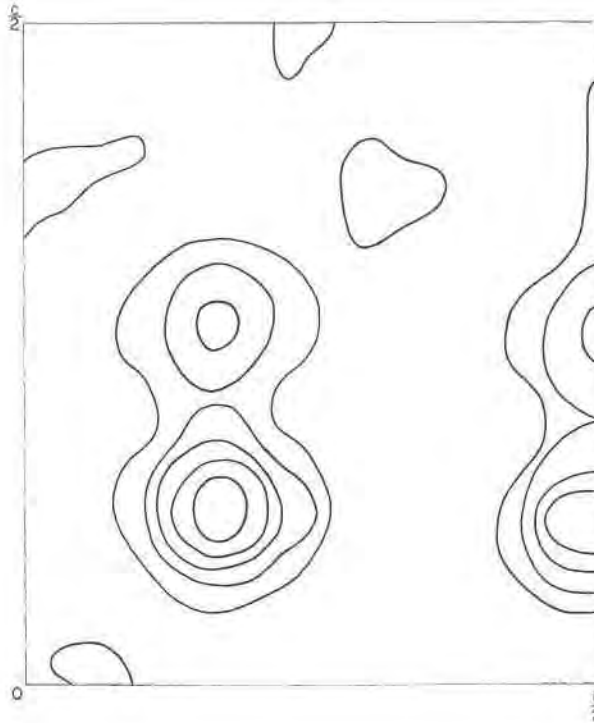

FIG. 3. Electron density projection, $\rho(yz)$, for cubanite.

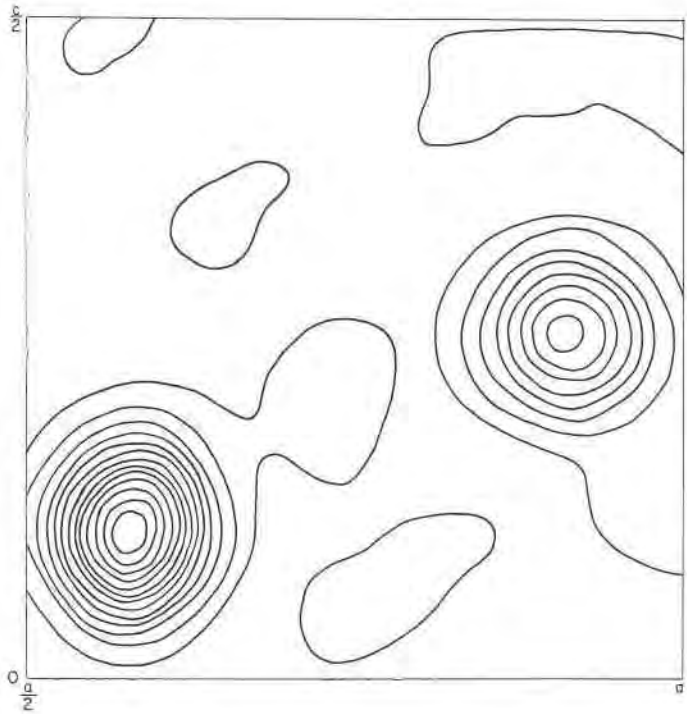

FIG. 4. Electron density section, $\rho(x\frac{1}{4}z)$, for cubanite.

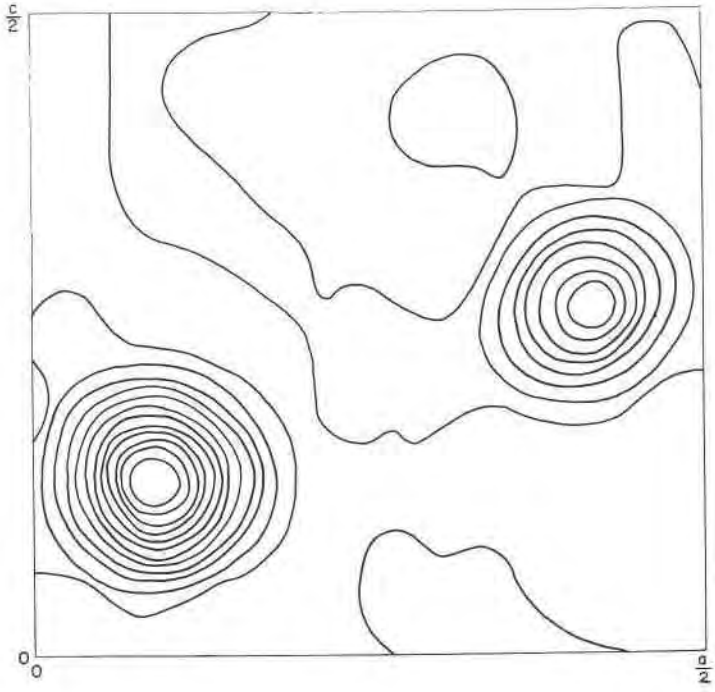

FIG. 5. Electron density section, $\rho(x\frac{1}{12}z)$, for cubanite.

projection $\rho(yz)$. In the second stage the full set of *hkl* intensities was used to pass strategically located plane sections through the atoms. In the third stage the full set of three-dimensional intensities was used to pass 3 orthogonal lines through each atom. This last stage of the refinement was carried out by difference syntheses. The refinement procedure is outlined in Table 1. This table not only gives the change of coordinates produced by each stage of the refinement but also the final values of the residual factor, $R=(\|F_o\|-|F_c|\|)/|F_o|$, at each stage of the refinement.*

Refinement by projections. The coordinates of the atoms resulting from the trial-and-error structure determination, and listed in Table 1, were used as a starting point. The phases determined by these coordinates were applied to the observed amplitudes, F_{okl}, and the electron density $\rho(yz)$ was computed. This is shown in Fig. 3.

The atoms are quite well resolved in this projection. The coordinates of the peaks found in $\rho(yz)$ were used to compute a new set of structure

* In computing R, F_o-F_c was omitted when $F_o=0$.

factors. None of these new structure factors showed any change in phase, which indicated that no further refinement was possible by successive Fourier projections. At this point the residual factor for the $0kl$ reflections was 19%.

Of the three projections of the electron density on the pinacoids, only the projection on (100) can show all of the atoms resolved from one another for the cubanite structure. This means that the end point of refinement by projections had been reached by the preparation of the $\rho(yz)$ synthesis. However, the new coordinates determined by this projection were used to compute the structure factors of the $hk0$ reflections. These proved to have the small residual factor of 9.7% which could hardly be improved.

Refinement by plane sections. The foregoing discussion makes it evident that any further refinement must come from employing all hkl reflections in some kind of three-dimensional Fourier synthesis. It will be observed from the tabulation of trial-and-error coordinates in Table 1 that the Cu and S_I atoms are confined to reflection planes with $y=\frac{1}{4}$, while the Fe and S_{II} atoms lie on planes having $y=.083\approx 1/12$. This makes it possible to refine the x and z parameters by passing plane sections through the structure at $y=\frac{1}{4}$ and $y=1/12$. Electron density syntheses corresponding to these sections were therefore prepared using

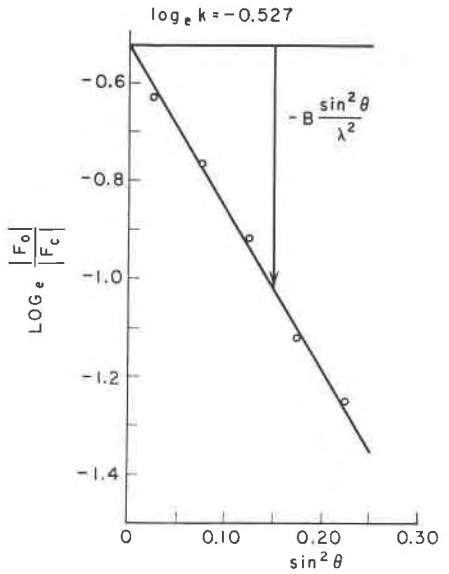

FIG. 6. Determination of absolute scale and temperature factor for cubanite.

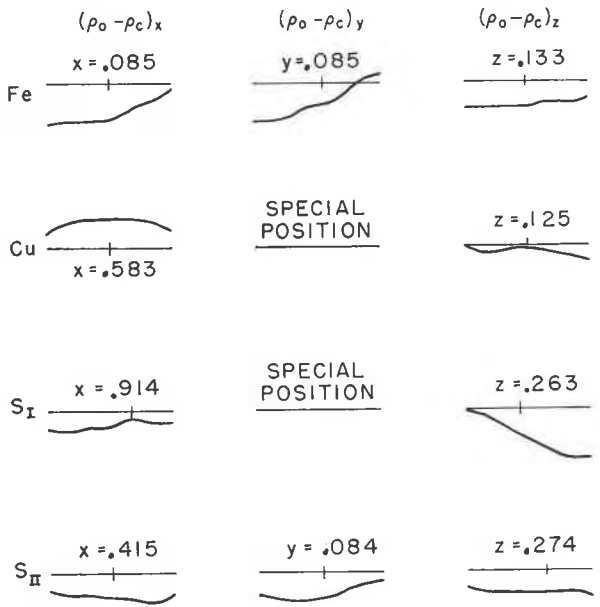

FIG. 7. First difference syntheses.

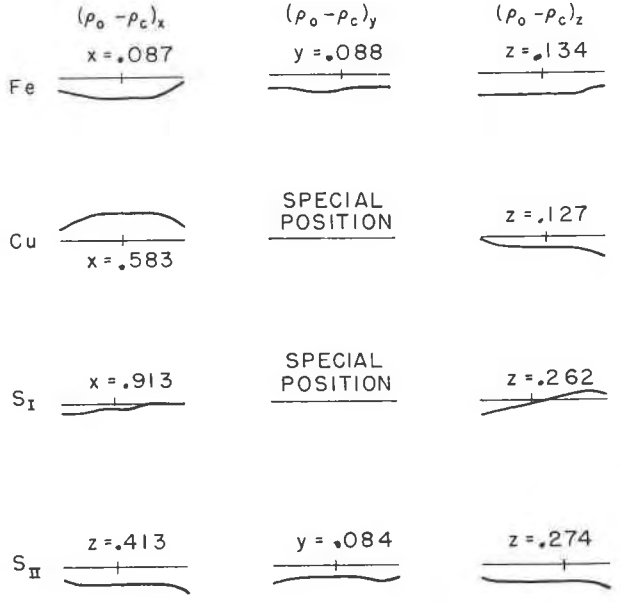

FIG. 8. Second difference syntheses.

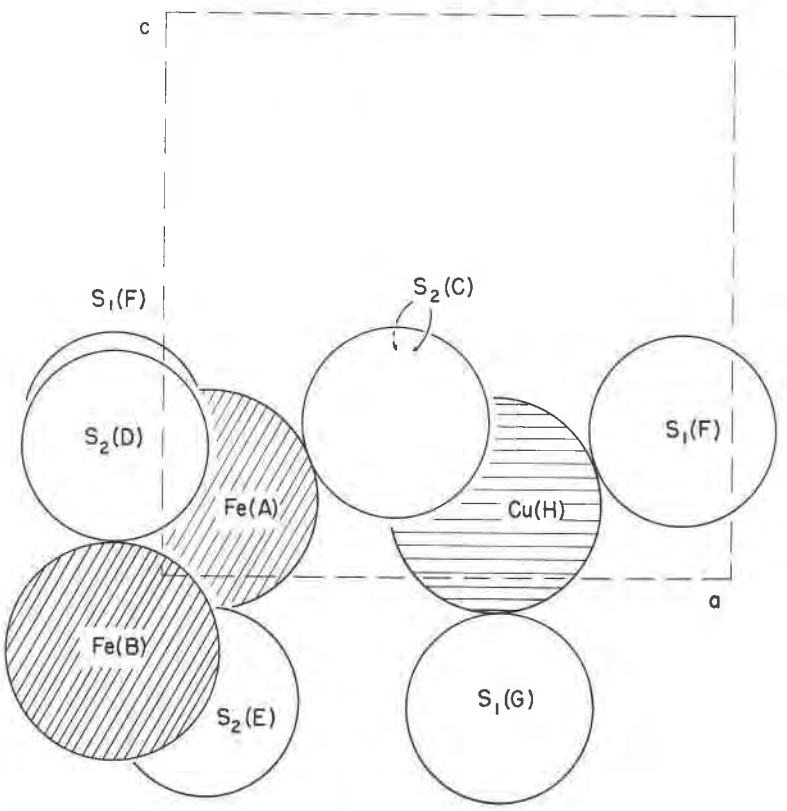

FIG. 9. Locations of atoms referred to in listing interatomic distances in cubanite.

the y and z parameters as refined by the projection $\rho(yz)$. These two syntheses are shown in Figs. 4 and 5. In these sections the atoms are clearly resolved. Their circular shapes suggest immediately that the phases are substantially correct. The coordinates obtained from these sections are tabulated in Table 1. The changes in coordinates over the last stage are very small indeed and correspond to no phase changes. The residual factor at this point for the entire three-dimensional set of intensities was 14%.

Refinement by difference syntheses. The shifts in atomic positions which had been encountered so far by the refinement procedure were so small that it could reasonably well be assumed that all atoms were near their final locations. The last stage in the refinement procedure was to study the atom locations as found in the foregoing stages by difference syntheses (Cochran, 1951). Since the atoms were substantially in their final positions, their centers could be readily located by passing three orthogonal lines (one parallel to each crystallographic axis) through each

TABLE 2. INTERATOMIC DISTANCES IN CUBANITE

Atom	Coordinates	Neighbor	Representative Coordinates	Bond Length
Fe(A)	x_1, y_1, z_1*	Fe(B)	$\bar{x}_1, \bar{y}_1, \bar{z}_1$*	2.80_8 Å
		S_2(C)	x_3, y_3, z_3	2.27_8 Å
		S_2(D)	$\frac{1}{2}+x_3, \bar{y}_3, \frac{1}{2}-z_3$	2.28_7 Å
		S_2(E)	$\frac{1}{2}-x_3, y_3, \frac{1}{2}+z_3$	2.24_5 Å
		S_1(F)	$x_4, \frac{1}{4}, z_4$	2.27_1 Å
Cu(H)	x_2, y_2, z_2	$2S_2$(C)	x_3, y_3, z_3	2.33_9 Å
		S_1(F)	$x_4, \frac{1}{4}, z_4$	2.29_2 Å
		S_1(G)	$\frac{1}{2}-x_4, \frac{1}{4}, \frac{1}{2}+z_4$	2.27_5 Å
S_2(C)	x_3, y_3, z_3	Fe(A)	x_1, y_1, z_1	2.27_8 Å
		Cu(H)	x_2, y_2, z_2	2.33_9 Å
		S_2(C)	$x_3, \frac{1}{2}-y_3, z_3$	3.70_2 Å
		S_2(E)	$\frac{1}{2}-x_3, y_3, \frac{1}{2}+z_3$	3.83_5 Å
		S_1(F)	$x_4, \frac{1}{4}, z_4$	3.72_4 Å
		S_1(G)	$\frac{1}{2}-x_4, \frac{1}{4}, \frac{1}{2}+z_4$	3.85_7 Å
S_2(D)	$\frac{1}{2}+x_3, \bar{y}_3, \frac{1}{2}-z_3$	Fe(A)	x_1, y_1, z_1	2.28_7 Å
		Fe(B)	$\bar{x}_1, \bar{y}_1, \bar{z}_1$	2.24_5 Å
		Fe	$\frac{1}{2}+x_1, \bar{y}_1, \frac{1}{2}-z_1$	2.27_8 Å
		S_2(C)	x_3, y_3, z_3	3.84_4 Å
		S_2(E)	$\frac{1}{2}-x_3, y_3, \frac{1}{2}+z_3$	3.61 Å
		S_1(F)	x_4, y_4, z_4	3.71_1 Å
S_1(F)	$x_4, \frac{1}{4}, z_4$	Cu(H)	$x_2, \frac{1}{4}, z_2$	2.29_2 Å
		Cu	$\frac{1}{2}-x_2, \frac{1}{4}, \frac{1}{2}+z_2$	2.27_5 Å
		2Fe(A)	x_1, y_1, z_1	2.27_1 Å
		S_2(E)	$\frac{1}{2}-x_3, y_3, \frac{1}{2}+z_3$	3.73_4 Å
		S_1(G)	$\frac{1}{2}-x_4, \frac{1}{4}, \frac{1}{2}+z_4$	3.76_2 Å

* The subscripts 1, 2, 3, 4 refer to the coordinates of Fe, Cu, S_{II}, S_I respectively, as tabulated in Table 1.

atom. Difference electron densities, $D=\rho_o-\rho_c$, were computed along each of these lines. The x and z coordinates used for ρ_c were thus given by $\rho(x\frac{1}{4}z)$ and $\rho(x\frac{1}{12}z)$ while the y coordinates were thus given by $\rho(yz)$. These coordinates were used to prepare computed values of the complete set of F_{hkl}'s. The ρ_o component of the synthesis was prepared by using observed F_{hkl}'s and the signs given by the computed F_{hkl}'s. The actual Fourier series were computed with the help of *ODFAC* (Azaroff, 1954), a one-dimensional computer built in this laboratory.

The criterion for the correctness of an atom location is that it should lie on the zero gradient of the difference synthesis. The first set of difference syntheses is shown in Fig. 7. Atoms lying on gradients were moved

TABLE 3. INTERATOMIC BOND ANGLES IN CUBANITE

Bonded Atoms	Angle
$S_2(D)$—Fe—$S_2(E)$	105° 36′
$S_2(C)$—Fe—$S_1(F)$	109° 57′
$S_2(C)$—Fe—$S_2(D)$	114° 44′
$S_1(F)$—Fe—$S_2(E)$	111° 35′
$S_2(C)$—Cu—$S_2(C)$	104° 38′
$S_2(C)$—Cu—$S_1(F)$	107° 03′
$S_1(F)$—Cu—$S_1(G)$	110° 54′
$S_2(C)$—Cu—$S_1(G)$	113° 12′

up the gradient and the second difference syntheses were prepared using these new coordinates. This second set is shown in Fig. 8. In this new difference synthesis all atoms appear to be on substantially zero gradient except for the z coordinate of S_I. In view of the fact that the gradient of the z difference synthesis for this atom changed direction it could be safely assumed that the atom lies between the parameter values assumed in computing these two sets of syntheses. The final set of parameters accepted for the structure is listed in the last column of Table 1. The R value had now been reduced to less than 12% for all hkl reflections. A comparison of observed and computed F values is now on file with the American Documentary Institute.*

INTERATOMIC DISTANCES IN THE STRUCTURE

The distances between atoms for the parameters found for the refined structure are listed in Table 2. In this table the designations (A), (B), etc., refer to the particular atoms so labelled in Fig. 9. The angles between the bonds are listed in Table 3.

It is interesting to examine the environment of the Fe atom (A). This atom is surrounded by four sulfur atoms, namely (C), (D), (E), and (F), at distances of 2.28, 2.29, 2.25 and 2.27 Å. The Fe atom (B), across the shared edge, is at a distance of 2.81 Å. This distance is longer than any of the customary Fe-Fe bond distances and yet much shorter than what would be expected if the Fe's were unbonded. The shared edge between these atoms has a length of 3.61 Å which is shorter than the other S-S distances (3.71, 3.72, 3.73, 3.84, and 3.84 Å) in the Fe tetrahedra. Ordinarily such a shortening of a shared edge would be attributed to an ionic component of the Fe atoms, but in this case it would appear

* A copy may be secured by writing to the *ADI Auxiliary Publications Project, Photoduplication Service, Library of Congress, Washington 25, D. C.*, and requesting Document number **4190.** Advance payment of $1.25 is required for photoprints, or $1.25 for 35 mm. microfilm. Make checks payable to: Chief, Photoduplication service, Library of Congress.

TABLE 4. CHARACTERISTICS OF COORDINATION TETRAHEDRA IN CUBANITE

Environment of Fe(A)	Environment of Cu(H)
S_2(E) 2.25 Å S_1(F) 2.27 S_2(C) 2.28 S_2(D) 2.29 Fe(B) 2.81	S_1(G) 2.28 Å S_1(F) 2.29 S_2(C) 2.34, 2.34
Tetrahedral Edges	**Tetrahedral Edges**
shared edge: 3.61 DE 3.71 DF 3.72 CF 3.73 EF 3.84 CD 3.84 CE	3.70 CC 3.72, 3.72 CF 3.76 FG 3.86, 3.86 CG

that a more reasonable interpretation is merely that it is due to the repulsion of those parts of the electronic clouds of the two atoms which are not involved in the Fe-Fe bond formation.

ACKNOWLEDGMENT

This research was supported by the Office of Naval Research under Contract No. *N5ori-07860* with the Massachusetts Institute of Technology.

REFERENCES

AZAROFF, LEONID V. (1954), A one-dimensional Fourier analogue computer: *Rev. Sci. Inst.*, **25,** 471–477.

BUERGER, M. J. (1944), The Photography of the Reciprocal Lattice. *ASXRED Monograph No.* **1.**

BUERGER, M. J. (1945), The structure of cubanite, $CuFe_2S_3$, and the coordination of ferromagnetic iron: *J. Am. Chem. Soc.*, **67,** 2056.

BUERGER, M. J. (1947), The crystal structure of cubanite: *Am. Mineral.*, **32,** 415–425.

BURBANK, R. D. (1952), Upper level precession photography and the Lorentz-polarization correction, Part I: *Rev. Sci. Inst.*, **23,** 321–327.

COCHRAN, W. (1951), The structures of pyrimidines and purines. V. The electron distribution in adenine hydrochloride: *Acta Cryst.*, **4,** 81–92.

DAWTON, R. H. V. M. (1938), The integration of large numbers of x-ray reflections: *Proc. Phys. Soc.*, **50,** 919–925.

EVANS, H. T., JR., and EKSTEIN, MIRIAM (1952), Tables of absorption factors for spherical crystals: *Acta Cryst.*, **5,** 540–542.

GRENVILLE-WELLS, H. J., AND ABRAHAMS, S. C. (1952), Upper level precession photography and the Lorentz-polarization correction, Part II: *Rev. Sci. Inst.*, **23,** 328–331.

WASER, J. (1951), The Lorentz factor for the Buerger precession method: *Rev. Sci. Inst.*, **22,** 567–568.

Manuscript received Jan. 20, 1954.